REPRINT

High quality In$_x$Ga$_{1−x}$N thin films with $x > 0.2$ grown on silicon

I. Gherasoiu[*,1], **K. M. Yu**[2], **L. A. Reichertz**[2], **V. M. Kao**[2], **M. Hawkridge**[2], **J. W. Ager**[2], **and W. Walukiewicz**[1,2]

[1] RoseStreet Labs Energy, Phoenix, Arizona, USA
[2] Materials Sciences Division, Lawrence Berkeley National Laboratory, Berkeley, California, USA

[*] Corresponding author: e-mail igheraso@yahoo.com, Phone: (602) 431-4782, Fax: (602) 437-1864

Using plasma-assisted molecular beam epitaxy (PA-MBE), high quality In$_x$Ga$_{1−x}$N layers with x in the range from 25 to 31% have been grown on silicon (111) substrates. The polarity of the layers has been found to impact the incorporation of In, with Ga polar buffers promoting the deposition of uniform composition InGaN. We have achieved films with indium fraction up to 31% and rocking curve width of 538 arcsec. Residual donor concentration as low as ~1.2×10^{18} cm^{-3} was measure in these films, suggesting that p-type doping with Mg can be achieved. The presence of AlN layers and the increasing thickness of the GaN buffer do not appear to have a significant contribution to the series resistance of the structure. The investigation of the InGaN layers by X-ray diffraction did not reveal any significant phase separation occurring during the MBE deposition although the photoluminescence spectrum exhibits low energy features that would require further investigation.

1 Introduction InGaN alloys are subject to an increasing research effort because of the continued application for light emitting devices, and high-efficiency solar cells [1, 2]. It has been found that the unusual band alignment between InGaN and Si can be exploited for the fabrication of tandem InGaN/Si heterojunction solar cells that may have power conversion efficiency higher than 30% [3]. Recently we have demonstrated the operation of a pn-GaN/pn-silicon tandem solar cell. Tandem nitride–silicon cells using InGaN alloys with In content up to ~45% for the top cell would absorb a larger portion of the terrestrial spectrum and provide a matched current for the silicon subcell. However, the growth of high crystalline quality In-rich InGaN has been found difficult by all deposition methods [4–7].

Although nanometer-thin InGaN layers are routinely grown by MOCVD on Al$_2$O$_3$ and SiC substrates for commercial optoelectronic devices, there are just few reports on the deposition of thick layers with indium composition larger than 20% [5, 6]. On silicon substrates, good quality GaN and InN layers have been reported [4], however, the growth of In$_x$Ga$_{1−x}$N films with $x > 0.1$ on silicon substrate remains a challenging task [7]. In this work, we report a systematic investigation of the growth and characterization of GaN and In$_x$Ga$_{1−x}$N alloys on Si (111) substrate with x up to 0.31.

2 Experimental All InGaN samples were grown on 4 in. Si (111) substrates using a production-style plasma-assisted molecular beam epitaxy (PA-MBE) system at RoseStreet Labs Energy in Phoenix, AZ. Five samples, A–E, have been produced under similar deposition conditions. The only difference between these samples was the thickness of the GaN buffer. Starting with sample A, the GaN thickness is 30, 90, 190, 410, and 640 nm. Elemental Al, Ga, and In were evaporated from Knudsen effusion cells while active nitrogen was generated using Veeco UNI-Bulb RF plasma sources. Typical nitride layers would consist of thin AlN buffer and a relatively thick (0.5 µm) GaN followed by InGaN of the desired composition deposited in the temperature range from 520 to 550 °C. *In situ* growth evolution was monitored continuously using a RHEED system and metal beam modulation has been employed for maintaining a good control over the material stoichiometry.

Film composition, thickness, and stoichiometry were evaluated by Rutherford backscattering spectrometry (RBS) while the crystallinity of the film was evaluated using ion channelling and high resolution X-ray diffraction (HRXRD). Microstructure and film polarity were determined by transmission electron microscopy (TEM). The free electron background was estimated based on the donor density

determined from electrochemical capacitance voltage (ECV) measurements while photoluminescence (PL) measurements were used to investigate the optical properties of the samples.

3 Results and discussion Figure 1 shows the comparison of channeling-RBS (c-RBS) result obtained from GaN layers grown on silicon (111) substrates (red trace) to that on a GaN template (black trace). The plot reveals that the crystalline quality of the GaN film grown on silicon is comparable to that of GaN layer grown directly on a GaN template under similar growth conditions. The high-channeling yield at the GaN/Si interface ($\sim$500 nm) arises from networks of misfit dislocations as confirmed by the TEM micrograph. The schematic of the nitride structure grown on silicon is depicted in the left side insert of Fig. 1.

TEM study confirms that the GaN layer is of high-crystalline quality with low-defect density and very sharp interfaces (right side insert of the Fig. 1). The typical residual donor concentration for these layers is in the range from low-10^{17} to mid-10^{16} cm^{-3}.

It has been previously shown that changing the growth conditions during the buffer growth could result in GaN layers that exhibit both polarities, Ga, or N [8]. The layer polarity has been reported to influence the surface morphology and more importantly, the impurity incorporation [9]. We have found that on N-polar layers, In incorporation in InGaN alloy is more difficult and In accumulation at the surface occurs, resulting in defective InGaN films with inhomogeneous In distribution. When the layers were Ga-polar GaN buffer, high-quality In$_x$Ga$_{1-x}$N films with x as high as 0.34 and sharp PL were successfully grown. Furthermore, residual donor concentrations in these films was determined in the range of high 10^{17} cm^{-3}.

The polarity of the GaN layers has been determined initially based on the surface reconstruction imaged with RHEED upon cooling of the sample below 400 °C. For N-polar samples the RHEED pattern along the 11$\bar{2}$0 azimuth shows a week 3× reconstruction, that has been reported
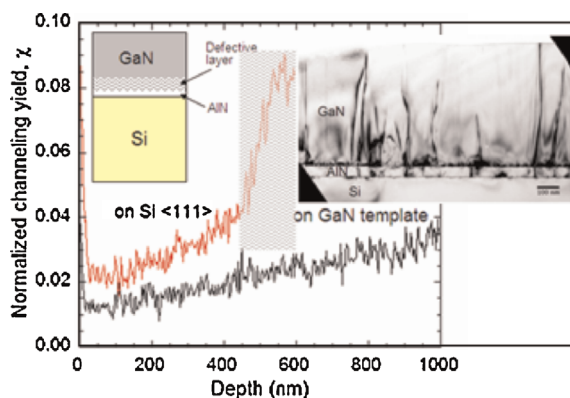
previously for MBE growth [10, 11]. Subsequent evaluation of the polarity performed using convergent beam electron diffraction (CBED) confirmed the N-polarity GaN layer.

Using growth conditions that have produced Ga-polar buffers, 100–170 nm thick In$_x$Ga$_{1-x}$N layers with indium fraction between 25 and 31% as estimated by RBS, were deposited on silicon. To avoid band edge discontinuities that are generated for a steep transition from the band gap of 3.4 eV of GaN to the lower band gap values of InGaN alloys centered around 2.3 eV, a graded InGaN layer has been used between the two regions. Five silicon substrates have been overgrown under similar conditions with GaN buffers having a thickness that increased gradually from 30 up to 640 nm. An improvement in the crystalline quality as revealed by HRXRD and ion channeling and a reduction in the residual donor concentration from 1.0×10^{19} to 1.2×10^{18} cm^{-3} is observed as the thickness of the GaN buffer layer increases from 30 nm (sample A) to 640 nm (sample E). A significant increase in channeling yields is seen for samples A and B with a buffer thickness below 100 nm, suggesting the loss of the lattice order.

The donor concentration appears to correlate well with the channeling yield data and could suggests that the InGaN crystallinity degradation may be associated with an increase in the number of donor point defects, either nitrogen vacancies (V$_N$) or impurities such as oxygen (O$_N$). Both defects introduce a shallow level at 32–37 meV bellow the conduction band [12] and have activation efficiency close to 100% [13, 14]. Also at this time, silicon out-diffusion originating from the substrate surface cannot be ruled out as a cause for the increased donor levels in the samples A and B. The determination of the specific series resistance, following the fabrication of contact pads did not reveal a trend that could be associated with thickness of GaN buffer. We conclude, therefore, that the contribution to the series resistance that is associated with this thickness is sufficiently low, such that other factors (i.e., contact resistance) dominate the overall behavior of the series resistance.

XRD spectrum from a typical InGaN film grown on Si is presented in Fig. 2 showing relatively narrow peaks for all nitride layers. A general trend of decreasing peak width (FWHM) is observed for both the GaN buffers and the InGaN layers as the buffer layer thickness increases. The values of the FWHM for the ω-scann, for GaN, and InGaN layers correlate very well with channeling yield at surface values provided by RBS. The density of the threading dislocations in the GaN and InGaN layers that may be a path of current leakage can be estimated from the peak broadening. For the GaN buffer layer and InGaN layer ($\sim$31% In) with the lowest FWHM value, we estimated an upper limit on the screw dislocation density to be 1.5×10^9 and 7.5×10^9 cm^{-2}, respectively.

A comparison of the variation of the c lattice spacing and the FWHM of the GaN buffer layer as a function of the GaN buffer thickness reveals that all the GaN buffer layers exhibit elongated c lattice spacing, above the threshold characteristic for relaxed material, indicative of the presence of

Figure 1 (online color at: www.pss-b.com) A comparison of the ion channeling results on a 600 nm thick GaN layer grown on the AlN buffer layer on Si (111) and a 600 nm GaN layer grown under similar growth condition on a GaN template layer on sapphire.

Phys. Status Solidi B **247**, No. 7 (2010)

1749
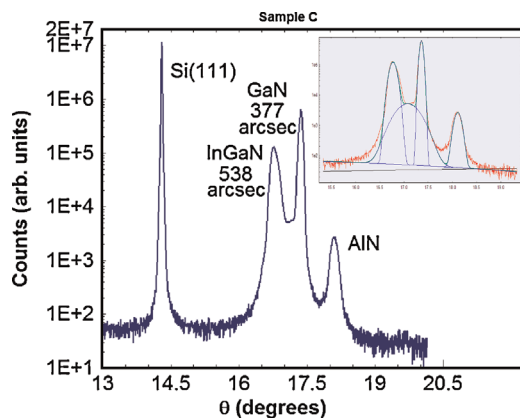
Figure 2 (online color at: www.pss-b.com) XRD spectra for (0002) reflection of the ω-scan. The inset shows the Gauss fit of the sample. The peaks represent the AlN, GaN, graded InGaN, and constant composition InGaN layers.

in-plane compressive stress. The evolution of the c lattice spacing suggests that the thin GaN layers are under an increased compressive stress that is released gradually with the increase of the GaN thickness.

A single well-defined 0002 diffraction peak attributed to the uniform InGaN layer is observed in the XRD pattern for all of our samples. No secondary peaks that could be attributed to clusters of higher InGaN composition can be observed. This suggests that no significant phase separation occurs during the MBE growth in the alloy composition region up to 31%. This observation is supported by RBS data as well, although the PL includes features consistent with the existence of small clusters of higher composition InGaN that have good luminescence properties. PL data are presented in Fig. 3. Alternately, the origin of these longer wavelength peaks has been attributed to the formation of extensive crystalline defects, staking faults, and edge segments of threading dislocations that are generated in the lower volume of the InGaN layer [15].
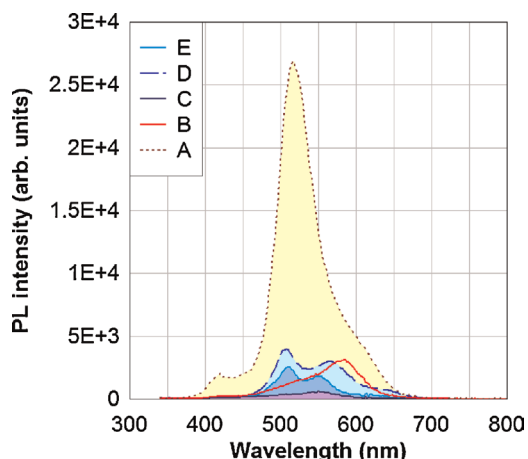
Figure 3 (online color at: www.pss-b.com) PL data for the InGaN samples. Samples A to E are in the order of increasing thickness of the GaN buffer.

4 Conclusions Using PA-MBE, high-quality $In_xGa_{1-x}N$ layers with x in the range from 25 to 31% have been grown on silicon substrates. We have achieved films with InN fraction up to 31% with rocking curve FWHM $\sim$540 arcsec. Residual donor concentration as low as $\sim$1.2 $\times$ 10^{18} cm^{-3} was measured in these films, suggesting that p-type doping with Mg can be achieved. The presence of AlN layers and the increasing thickness of the GaN buffer do not appear to have a significant contribution to the series resistance of the structure. We believe that the electrical, optical, and structural properties of these films allow us to fabricate our proposed InGaN-Si hybrid tandem solar cell.

References

[1] L. Hsu and W. Walukiewicz, J. Appl. Phys. **104**, 024507 (2008).

[2] J. Wu, W. Walukiewicz, K. M. Yu, W. Shan, J. W. Ager, III, E. E. Haller, H. Lu, W. J. Schaff, W. K. Metzger, and S. Kurtz, J. Appl. Phys. **94**, 6477 (2003).

[3] J. W. Ager, III, L. A. Reichertz, D. Yamaguchi, L. Hsu, R. E. Jones, K. M. Yu, W. Walukiewicz, and W. J. Schaff, Group III-nitride alloys for multijunction solar cells, in: Proceedings of 22nd European Photovoltaic Solar Energy Conference and Exhibition, Milan, Italy, 2007.

[4] C.-L. Wu, C.-H. Shen, H.-Y. Chen, S.-J. Tsai, H.-W. Lin, H.-M. Lee, S. Gwo, T.-F. Chuang, H.-S. Chang, and T. M. Hsu, J. Cryst. Growth **288**, 247 (2006).

[5] B. N. Pantha, J. Li, J. Y. Lin, and H. X. Jiang, Appl. Phys. Lett. **93**, 182107 (2008).

[6] D. Iida, M. Iwaya, S. Kamiyama, H. Amano, and I. Akasaki, Appl. Phys. Lett. **93**, 182108 (2008).

[7] Y. E. Romanyuk, D. Kreier, Y. Cui, K. M. Yu, J. W. Ager, III, and S. R. Leone, Thin Solid Films **517**(24), 6512–6515 (2009).

[8] D. Huang, P. Visconti, K. M. Jones, M. A. Reshchikov, F. Yun, A. A. Baski, T. King, and H. Morkoc, Appl. Phys. Lett. **78**(26), 4145–4147 (2001).

[9] F. Tuomisto, K. Saarinen, B. Lucznik, I. Gregory, H. Teisseyre, T. Suski, S. Porowski, P. R. Hageman, and J. Likonen, Appl. Phys. Lett. **86**, 031915 (2005).

[10] L. K. Li, M. J. Jurkovic, W. I. Wang, J. M. Van Hove, and P. P. Chow, Appl. Phys. Lett. **76**(13), 1740–1742 (2000).

[11] E. S. Hellman, MRS Internet J. Nitride Semicond. Res. **3**, 11 (1998).

[12] D. Steigerwald, S. Rudaz, H. Liu, R. S. Kern, W. Götz, and R. Fletcher, JOM **49**(9), 18–23 (1997).

[13] O. Brandt, H. Yang, J. R. Mullhauser, A. Trampert, and K. H. Ploog, Mater. Sci. Eng. B **43**, 215 (1997).

[14] M. Rummukainen, J. Oila, A. Laakso, K. Saarinen, A. J. Ptak, and T. H. Myers, Appl. Phys. Lett. **84**(24), 4887–4889 (2004).

[15] N. Faleev, B. Jampana, A. Pancholi, O. Jani, H. Yu, I. Ferguson, V. Stoleru, R. Opila, and C. Honsberg, 33th IEEE Photovoltaic Specialists Conference 2008.